RI 8316

Bureau of Mines Report of Investigations/1978

Radon Daughter Mixture Distributions in Uranium Mine Atmospheres

UNITED STATES DEPARTMENT OF THE INTERIOR

Report of Investigations 8316

Radon Daughter Mixture Distributions in Uranium Mine Atmospheres

By Robert F. Holub and Robert F. Droullard

UNITED STATES DEPARTMENT OF THE INTERIOR
Cecil D. Andrus, Secretary

BUREAU OF MINES

This publication has been cataloged as follows:

Holub, Robert F

Radon daughter mixture distributions in uranium mine atmospheres / by Robert F. Holub and Robert F. Droullard. [Washington] : U.S. Dept. of the Interior, Bureau of Mines, 1978.

20 p. : diagrs. ; 27 cm. (Report of investigations - Bureau of Mines ; 8316)

Bibliography: p. 19-20.

1. Radon. 2. Uranium mines and mining - Safety measures. I. Droullard, Robert F., joint author. II. United States. Bureau of Mines. III. Title. IV. Series: United States. Bureau of Mines. Report of investigations - Bureau of Mines ; 8316.

TN23.U7 no. 8316 622.06173

U.S. Dept. of the Int. Library

CONTENTS

ILLUSTRATIONS

TABLES

RADON DAUGHTER MIXTURE DISTRIBUTIONS IN URANIUM MINE ATMOSPHERES

by

Robert F. Holub [1] and Robert F. Droullard [2]

ABSTRACT

The Bureau of Mines has made a study of the magnitude of the variations of radon daughter mixtures, with the objective of determining whether these variations reflect the existing physical conditions in uranium mine atmospheres or if they are merely random or systematic errors. To accomplish this, many data have been plotted using a triangular graphing technique which shows that plateout affects RaA more than RaB or RaC, and that it is impossible to find simple correlations between working level ratios, radon daughter mixtures, and age.

INTRODUCTION

Studies of radon daughter air concentration measurements show that mixtures of RaA, RaB, and RaC vary in an unrecognizable manner. Factors affecting these daughter product mixtures have been studied by several investigators (1-2, 6, 10),[3] but the results appear to be inconclusive. This study explores several factors having an influence on the results of measurements of RaA, RaB, and RaC in mine atmospheres such as measurement method errors, constancy of daughter concentrations during the sampling time, daughter growth models, and daughter plateout.

Measurement methods influence the error propagation owing both to counting statistics and to some possible contaminants or losses of activity. The constancy of radon daughter concentrations during sampling time is a standard assumption; it is very likely that if this assumption is not justified, some errors will be introduced.

A growth model is an idealized time development of radon daughter concentrations in systems containing air, radon, and airborne radon daughters.

---

[1] Health physicist.

[2] Supervisory geophysicist.

Both authors are with the Denver Mining Research Center, Bureau of Mines, Denver, Colo.

[3] Underlined numbers in parentheses refer to items in the list of references at the end of this report.

There are three growth models for an enclosed volume: (1) ventilated with constant radon emanation, (2) unventilated with continuous radon emanation, and (3) unventilated with initial radon concentration. If fresh radon is constantly supplied to a system, the instantaneous radon daughter concentration will differ from the concentration of a system that has no fresh radon supply. Likewise, the introduction of fresh air to a system will also have a substantial effect on the radon daughter concentration.

To gain some insight into the problem, about 400 published measurements taken by different groups over the past 15 years have been plotted and analyzed.

Another purpose of this work is to demonstrate a new and convenient, two-dimensional way of plotting the radon daughter mixtures. Using this approach, the disadvantages of the common one-dimensional plot are eliminated, more data can be plotted on one graph, and more physical relationships can be ascertained.

There are three radon daughters to plateout or change their concentration before or during the sampling, which results in a multivariate statistical problem. However, it is beyond the scope of the present investigation to try to unravel these naturally dependent statistical variables since it would require, in the most general case, a determination of 9 standard deviations and up to 36 correlation coefficients.

DESCRIPTION OF THE PLOTTING METHOD

The basis of the plotting is the triangular graph used in figures 1-4. Any point within the triangle represents an airborne activity mixture of radon daughters normalized to 1 working level (WL). The lower left corner represents pure RaA with an activity of 956.3 picocuries, the upper right corner represents pure RaB with an activity of 193.9 picocuries, and the upper left corner represents pure RaC with an activity of 263.7 picocuries. Zero activity for RaA and RaB is at the upper left corner, while zero activity for RaC is on the hypotenuse side of the triangle. For simplicity the RaC axis, which is on the perpendicular bisector of the hypotenuse, is not shown on any of the figures. These triangular graphs were used previously in references 3 and 5.

Prior to a detailed discussion of the data points, the following basic features should be noted: (1) any data appearing in or near the lower left corner correspond to young air,[4] and (2) very old air is in the region where RaA, RaB, and RaC have activities of about 100 picocuries (the equilibrium point). The curve drawn from the lower left corner to the equilibrium point describes the time development of the radon daughter mixtures from an initially pure radon which is a radon growth model 3 to be discussed later. The equilibrium point is reached in about 3 hours; thereafter, the daughter concentrations do not change. The classical radon daughter growth curve,

[4] Young air is air containing radon but low concentrations of daughters because there has not been enough time for them to develop. Old or equilibrium air is air with radon and daughter concentrations approaching equilibrium conditions.

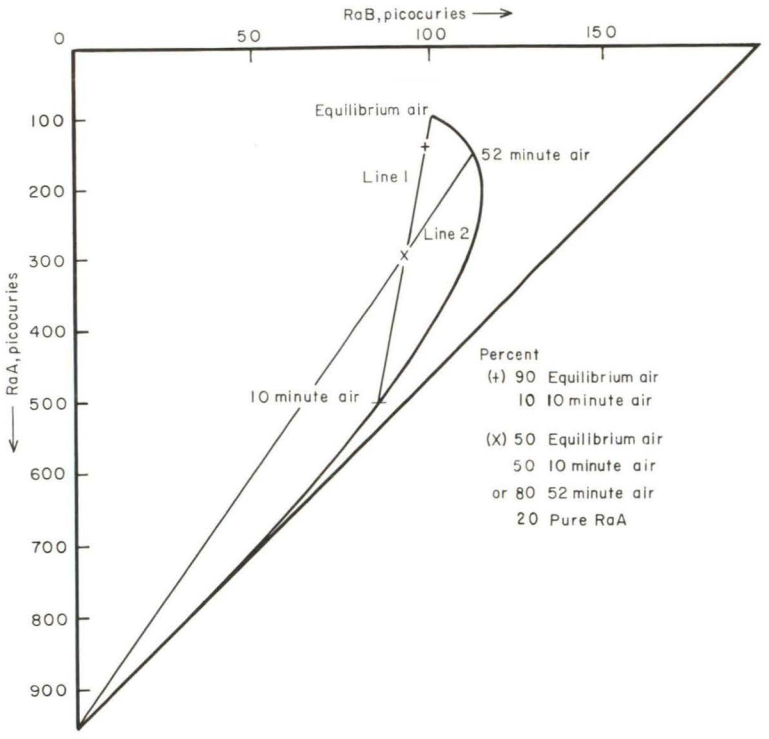

FIGURE 1. - A two-dimensional plot showing the construction of mixtures of various ages of air.

growth model 3, is provided as a reference for the data plotted.

Another convenient feature of these graphs is the ease with which the mixtures of various ages of air and models can be constructed. An example is shown in figure 1 where the composition of points are being determined. The first step is to draw straight lines through these points and some other points chosen as possible components. It should be noted that any straight line may be drawn between any two different points (or ages) to form a set of mixtures almost anywhere in the domain of the measured data points. The chosen components do not have to lie only on the curve drawn in figure 1 (growth model 3); they may lie on any curve corresponding to growth models 1 and 2. In the example in figure 1 the components are:

1. Equilibrium air and air 10 minutes old (line 1). These two components could be derived from an injection of air 10 minutes old into an air that was traveling through a mine tunnel for 3 hours.

2. Air 52 minutes old and absolutely young air with pure RaA (line 2). This is not a likely combination, but it does illustrate the point.

The second step is to measure where the points lie on the straight lines. Point + on line 1 is at one-tenth of the whole length between the point corresponding to 10 minute air and to equilibrium air, which can be described as a mixture of 90 percent equilibrium air and 10 percent air 10 minutes old. The remaining possibilities are listed in figure 1.

To show the location of line 1 in relation to the data points, it is also drawn in figures 2-3 as a full line. The dashed line is for the components of equilibrium air and the pure RaA concentration point on the graph.

The data points have been plotted using a simple computer program and the actual plotting in figures 2-3 was done by an X-Y plotter.

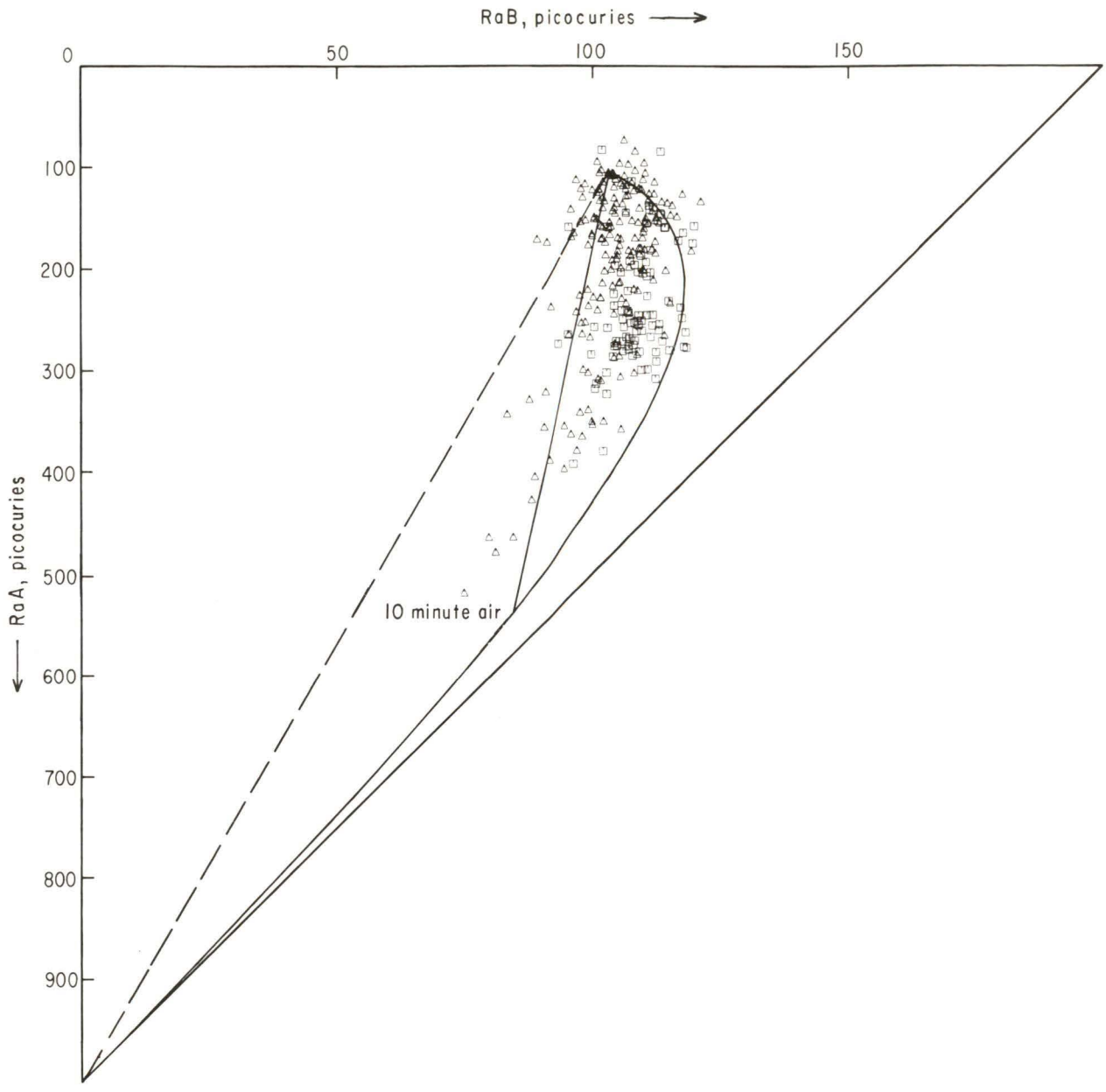

FIGURE 2. - A two-dimensional plot of 275 data points whose value exceeds 0.5 WL.

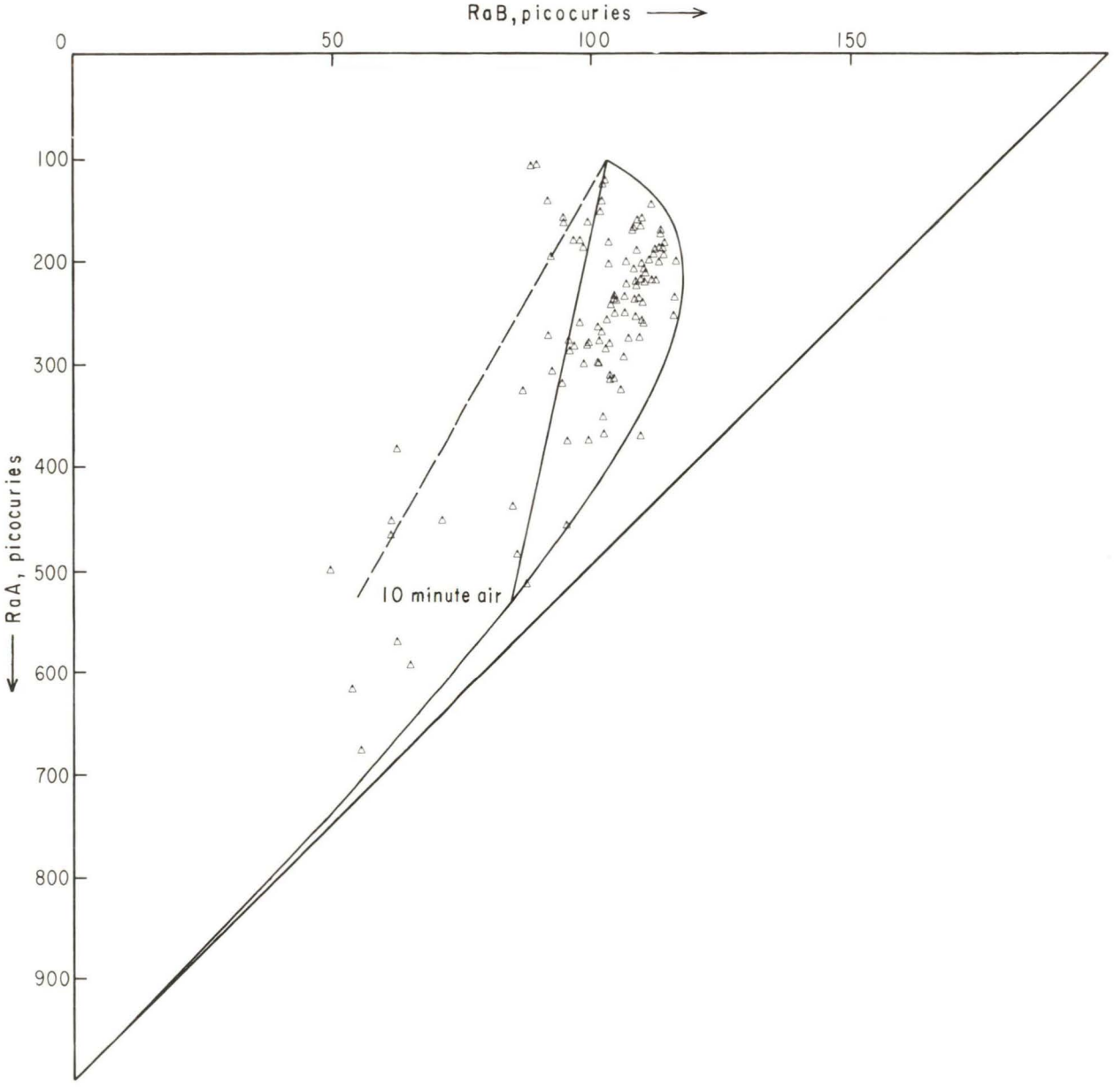

FIGURE 3. - A two-dimensional plot of 105 data points whose value is less than 0.5 WL.

RESULTS

Figure 2 contains 275 data points whose WL value exceeds 0.5. Of these, 170 are data compiled by Lovett (6) labeled △ and the rest are data labeled ⊡, measured by the Radiation Branch, Denver Technical Support Center, Mining Enforcement and Safety Administration (MESA),[5] Denver, Colo. (9), or the

[5]MESA became the Mine Safety and Health Administration (MSHA), U.S. Department of Labor, on Mar. 9, 1978.

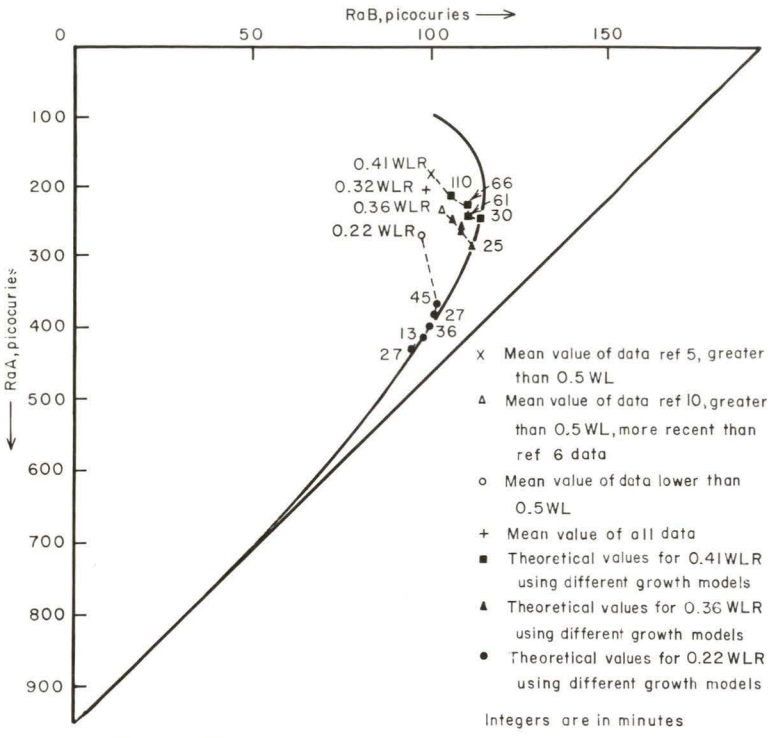

FIGURE 4. - The disagreement of the theoretical "ages of air" as inferred from the radon daughter growth models and the average experimental mixture locations of the data. The integers are in minutes.

Bureau of Mines. The mean working level value for the Lovett data is plotted in figure 4, and is labeled X; the mean value for the MESA data is labeled Δ.

Figure 3 contains 105 data points with WL values less than 0.5. Most of these data are from the Lovett compilation. Their mean value, labeled o, is plotted in figure 4. The mean value of all 385 data, labeled +, is also plotted in figure 4.

Most of the data plotted in figures 2-4 have been obtained using the modified Tsivoglou method (11).

About 80 percent of the data measured include the radon concentration. This enables the calculation of the working level ratio (WLR), which is defined as 100 times the WL divided by the radon concentration in picocuries per liter. At equilibrium, the mixture has an activity of 100 picocuries per liter for all daughters of 1 working level and the WLR has a value of 1.0. In general, it is considered "a convenient, if approximate, unit expressing the degree of equilibrium between gas and its daughters" (1). To check this assumption, the mean values of working level ratios for various sets of data were compared with several ages in table 1 and figure 4. The ages are inferred from various growth models to be described later. The mean values for the radon daughter mixtures normalized to 1 WL are given in the first three columns of table 1 and the corresponding locations are given in figure 4. The ages were calculated for the given WLR values; they are given in figure 4 in minutes. Those for WLR = 0.41 are labeled ■; for WLR = 0.36 are labeled ▲; for WLR = 0.22 are labeled ●. To facilitate understanding, the experimental and the theoretical points belonging to the same WLR are connected by the dashed lines.

The important consequences of the same WLR value having so many different locations on the graph will be discussed in the "Discussion" section.

TABLE 1. - Comparisons of the ages as inferred from WLR measurements for different radon daughter growth models

Data description	Mixtures normalized to 1 WL, pC/1			WLR, average	Radon daughter growth model age, minutes				
	RaA	RaB	RaC		[1]3	[1]2	[1]1 [2]360	[1]1 [2]45	[1]1 [2]20
Concentrations greater than 0.5 WL:									
Lovett's compilation (shown in figure 4 as X).....	186	101	75	0.41	30.0	61.1	66.0	110	Out of range.
MESA measurements (shown in figure 4 as Δ).....	225	105	58	.36	25.0	52.0	53.0	75	Out of range.
Concentrations smaller than 0.5 WL: All measurements (shown in figure 4 as o)..	255	97	60	.22	13.5	27.5	27.5	31	45
Total (shown in figure 4 as +).....	221	101	66	.32	21.0	44.0	44.0	56	Out of range.

[1] Numbers refer to the growth model (as used in reference 1).
[2] Number of minutes refer to durations during which a complete air exchange takes place.

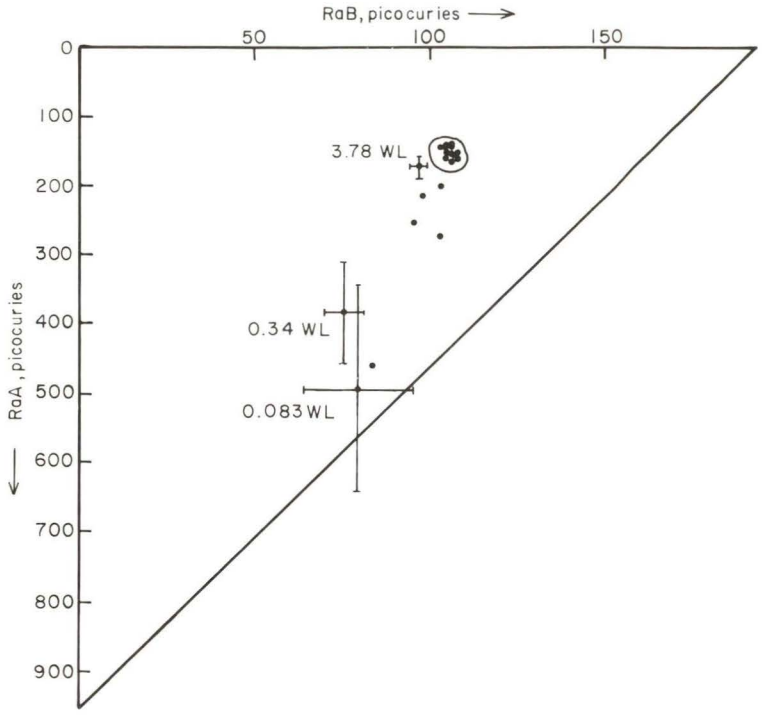

FIGURE 5. - Bureau of Mines mine measurements under various conditions. The error bars are the counting statistics errors for a given WL.

In figure 2, a straight, dashed line is drawn from the pure RaA point to the equilibrium point. The area enclosed on one side by this line and by the growth model 3 curve on the other side is defined in this paper as the "natural domain" of radon daughter mixtures.

Data taken by the Denver (Colo.) Mining Research Center are plotted in figure 5. It shows the influence of unsteady conditions on the spread of the data. The error bars shown for some points correspond with counting statistics errors as calculated according to Thomas (11). It should be also noted that in figures 2-3 a substantial percentage of the data (approximately 60 data points) lie outside the region defined previously as the natural domain of radon daughter mixtures which will be discussed later.

DISCUSSION

The most striking feature in figures 2-3 is the spread and the elongated shape of the data distribution. It is the main subject of this section to discuss and explain this spread and shape. There are five main effects which determine the data location on the graph.

1. Counting statistics.

2. All other errors.

3. Nonconstancy of the daughter concentration during sampling.

4. Radon daughter growth models.

5. Plateout.

Counting Statistics

Before starting to track down some real physical relationships, it must be made certain that counting statistics and other errors are not the main culprits causing the spread of data. Breslin and others (1) plotted experimentally determined statistical errors for both Kusnetz and the old Tsivoglou method (1, p. 30). Later Martz and others (7) derived a theoretical evaluation, using the standard formulas for error propagation for RaA, RaB, and RaC standard deviations, and later, the same approach was used by Thomas (11) for the modified Tsivoglou method. The results of these calculations, after some modifications for RaA, RaB, and RaC in dependence on WL, are plotted in figure 6. The individual curves are: (1) full line, RaA for an equilibrium mixture of 100 picocuries for all daughters; (2) dashed line, RaA for the mixture of 320:125:25 picocuries per liter; and (3) full lines close together representing RaB and RaC. It is not necessary to plot the last two curves for

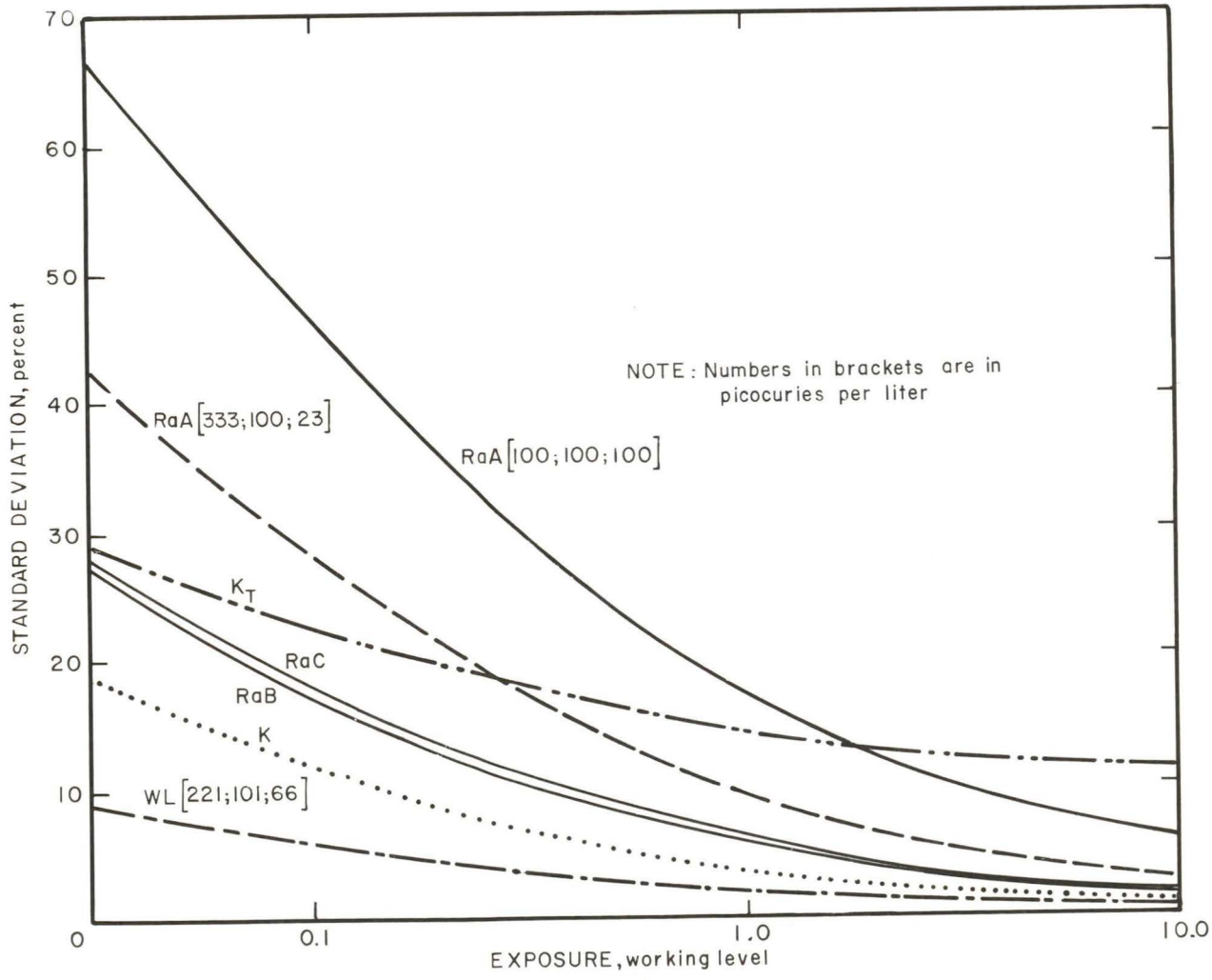

FIGURE 6. - Counting statistics errors for radon daughters and working levels for various mixtures (given in the square brackets) in dependence on the working levels.

different mixtures because they are practically independent of the radon daughter mixtures. The remaining curves will be described later.

The counting statistics errors for RaA and RaB are also shown as error bars in figure 5, together with the values for the working levels 0.083, 0.34, and 3.78. Using standard error propagation methods, the error for WL has been calculated. The resulting standard deviations for WL (σ_{WL}) in WL units, using reference 11 notation, sampling and counting times, is as follows:

$$\sigma_{WL} = \frac{1.7349 \times 10}{V\,E}\left(31.51\ I_{2,5} + 0.634\ I_{6,20} + 121.4\ I_{21,30} + \frac{3939}{T_B}\ R\right)^{1/2}, \quad (1)$$

where V = the air sampling rate in liters per minute,

E = counting efficiency,

I_{T_1,T_2} = number of alpha counts, uncorrected for background, from T_1 to T_2 minutes after the end of sampling,

T_B = background counting time in minutes,

and R = background counting rate in counts per minute.

The corresponding (dash-dot) curve is plotted in figure 6. The "most probable mixture" or the "midpoint mixture" has been chosen as (221:101:66). It has been found that mixture fluctuations do not have much effect on the σ_{WL} value.

The standard deviation for WL is lower than the standard deviations for RaA, RaB, and RaC due to favorable error propagation relationships.

A comparison with a corresponding Kusnetz WL measurement,[6] based on one measurement and with the standard deviation proportional to the square root of the count, a 5-minute sampling period and a measurement time at 40 minutes after the end of sampling (5), gives the results shown in figure 5 (dotted line-curve K). For these results to be comparable with the Tsivoglou measurements, the same efficiency (0.467) and a counting time similar (10 minutes) to the Tsivoglou method have been chosen.

To be complete, the Kusnetz inherent error for data points falling within the most probable region has been added (curve K_T, dash-dot-dot-line) to the statistical counting error for the Kusnetz method.

The errors plotted in figure 6 are lower than those reported by Breslin and others (1) because they did not use the modified Tsivoglou method. According to Thomas (11), the improvement of the accuracy should be almost a factor of 3 for RaA, RaB, and RaC when his method is used. To explain the accuracy of the modified Tsivoglou method being from three to five times better than

[6] Most Kusnetz measurements are done with a counting time of 1 minute and an efficiency of about 30 percent.

the original Tsivoglou method, note three measurements are used while the Kusnetz method uses only one; therefore, the former is, in a sense, an average of three measurements. Figures 5-6 permit determination of the counting statistics errors.

Other Errors

When investigating the spread of data normalized to 1 WL, only factors that influence the daughter mixtures and not the value of the working levels need to be considered. For example, the accuracy of the airflow measurements are of no consequence because they affect all radon daughters the same way. Two errors associated with counting that could favor a particular daughter are self-absorption in the filter paper and the presence of thoron daughters or the RaD, RaE, RaF chain. RaF (Po-210) is an alpha emitter which is long-lived and by adding an alien activity, makes the Tsivoglou equations erroneous. Because these two errors could be serious, self-absorption was checked both theoretically and experimentally. The effect of long-lived activity was evaluated theoretically.

To test the effects of self-adsorption of the filters, three measurements were made using a membrane-type filter where self-absorption is minimal and three measurements were made using a standard fiberglass filter. It was assumed, on the basis of previous experience, that the mixtures have not changed significantly during this period. The mean values of these tests are given in table 2. The method of measurement used is the modified Tsivoglou, and the nomenclature is that used by Thomas.

TABLE 2. - Measured and calculated differences between the Rn daughter concentrations without and with self-absorption

Experimental	Counts per minute			Picocuries per liter			
	$I_{2,5}$	$I_{6,20}$	$I_{21,30}$	RaA	RaB	RaC	WL
Membrane filter paper..	17,493	50,954	27,561	1,147	452	189	4.25
Fiberglass filter paper	16,348	48,298	27,241	1,049	430	183	4.02
Difference between.....	-1,145	-2,655	-315	-98	-22	-5	-0.23
Percent.....	6.5	5.0	1.0	8.5	5.0	2.5	5.5
Calculated:							
Case 1.....	NAp	NAp	NAp	-181	5	18	
Case 2.....	NAp	NAp	NAp	-10	-35	-24	
Average.....	NAp	NAp	NAp	-96	-15	-3	

NAp Not applicable.

The results of the preceding experimental work can also be illustrated theoretically by small subtractions from the basic equations for RaA, RaB, and RaC, as they are given in reference 11. Each of the three measurements ($I_{2,5}$, $I_{6,20}$, $I_{21,30}$, where 2,5; 6,20; and 21,30 are the times of the beginning and the end of these measurements after end of sample period) consists of RaA and RaC' alpha particles. It is difficult to estimate the loss of activity due to self-absorption for RaA and RaC individually. Since the nature of these

considerations is only approximate, it was considered acceptable to choose two extreme cases (labeled case 1 and case 2), which, even though they cannot happen in nature, provide a lower and upper limit.

Case 1.--In this case the decrease in activity due to self-absorption of RaA is estimated. From reference 11, equations can be written for RaA, RaB, and RaC (labeled C_2, C_3, and C_4), with the small subtractions for RaA, $\Delta IA_{2,5}$, and disregarding the sampling flow rate and efficiency, as

$$C_2 = 0.1689\ (I_{2,5} - \Delta IA_{2,5}) - 0.082\ (I_{6,20} - \Delta IA_{6,20}) + 0.0775\ (I_{21,30} - \Delta IA_{21,30}), \quad (2)$$

$$C_3 = 0.0012\ (I_{2,5} - \Delta IA_{2,5}) - 0.0206\ (I_{6,20} - \Delta IA_{6,20}) + 0.491\ (I_{21,30} - \Delta IA_{21,30}), \quad (3)$$

and

$$C_4 = 0.02251\ (I_{2,5} - \Delta IA_{2,5}) + 0.0332\ (I_{6,20} - \Delta IA_{6,20}) - 0.0377\ (I_{21,30} - \Delta IA_{21,30}). \quad (4)$$

The RaC component does not change very much in activity throughout the three measurements. This approximation is based on the realization that the decay of RaC' is complemented by the decayed RaB. Also note that

$$\Delta IA_{21,30} \simeq 0,$$

because of the RaA short half-life and

$$\Delta IA_{6,20} = \Delta IA_{2,5} \exp(-\lambda_{RaA} t) = \Delta IA_{2,5}\ 0.052,$$

where λ_{RaA} and t are the RaA decay constant and elapsed time from the first measurement.

The next step is to look at partial derivatives of the RaA, RaB, and RaC activities with respect to the small subtraction, ΔIA. When the differences in the counting times for the individual measurements are approximately taken into account, the results are

$$\frac{\delta C_2}{\delta \Delta IA_{2,5}} = -0.149, \quad (5)$$

$$\frac{\delta C_3}{\delta \Delta IA_{2,5}} = 0.0083, \quad (6)$$

and

$$\frac{\delta C_4}{\delta \Delta IA_{2,5}} = 0.0144. \quad (7)$$

When the preceding numbers are used for the case shown in table 2, using the expressions

$$\Delta C_2 = -0.149\ \Delta IA_{2,5}, \tag{8}$$

$$\Delta C_3 = 0.0038\ \Delta IA_{2,5}, \tag{9}$$

and

$$\Delta C_4 = 0.0144\ \Delta IA_{2,5}, \tag{10}$$

where ΔC_1 is the difference in Rn daughters concentration due to small subtraction $\Delta IA_{2,5}$, the results shown at the bottom of table 2, case 1 are found.

Case 2.--In this case the decrease in activity due to self-absorption of RaC', which is in general different than for RaA, is estimated. As mentioned previously, the RaC' contribution to the three counting periods of the modified Tsivoglou method can be considered constant. For this reason the notation $\Delta IC_{T_1 T_2}$ is chosen which indicates a small contribution to the count I due to RaC' for any of the three counting periods. Using the same equations as before, the following results are found:

$$\frac{\delta C_2}{\delta \Delta IC_{T_1 T_2}} = 0.0087, \tag{11}$$

$$\frac{\delta C_3}{\delta \Delta IC_{T_1 T_2}} = 0.0523, \tag{12}$$

$$\frac{\delta C_4}{\delta \Delta IC_{T_1 T_2}} = 0.0194. \tag{13}$$

Using these numbers in the same way as in equations 8, 9, and 10, the numbers presented in table 2 as case 2 are found.

A closer look at table 2 can give the following useful information about the effect of small subtractions[7] from the true values:

1. While there is, for instance, an 8.5 percent lower concentration of RaA, when normalized to 1 WL, the difference in a position on the graphs of figures 1-2 is only about 2 percent. It is, therefore, very unlikely that the points that are outside the natural domain can be accounted for by researchers using alpha-absorbing filter papers and similar oversights. Only self-absorption or deadtime losses at least two to three times higher than those shown in table 2 could account for some of the shifts outside the natural domain, which seems quite unlikely.

2. The average of the calculated values given in table 2 (cases 1 and 2) agree reasonably well with the experimentally found values, which provides additional confidence in the approximate calculations and the conclusions.

[7] The subtractions can come not only from self-absorption but also from not applying deadtime corrections.

The remaining case (a constant activity ΔI as a small addition to the true activity of the daughters in all three measurements) gives the following results:

$$\frac{\delta C_2}{\delta \Delta I} = 0.0087, \tag{14}$$

$$\frac{\delta C_3}{\delta \Delta I} = 0.0523, \tag{15}$$

and

$$\frac{\delta C_4}{\delta \Delta I} = 0.0194. \tag{16}$$

These expressions show how the daughter activities increase with constant activity which could result from the long-lived thoron daughter or Po-210 activities. The latter activity could be present on dust in uranium mines. In our measurements it was found on several occasions that there are long-lived activities which rarely exceed 1 percent of the total. However, it is conceivable they could be higher in some mines.

From the preceding, it can be seen that a constant activity addition is going to move the points in the triangular graphs in the direction of increased RaB (the partial derivative for RaB (C_3) is largest and is positive). It will not be in the direction of decreased RaA; therefore, this effect cannot explain the data in figures 1-2 which have a very low RaA component.

Nonconstancy of the Daughter Concentration During Sampling

This appears to be an entirely neglected subject. From the work published on cave breathing (12), in response to changes in pressure and temperature, it may be safely concluded that in a naturally ventilated mine the flow can be changed substantially or even reversed several times during a day. Sometimes these changes in concentration are called "gusts" of radon and radon daughters. The quoted work does not mention ventilated caves; however, it should be first proved that in such cases the concentration is constant rather than to assume it.

Radon Daughter Growth Models

The most common explanation of the spread of the data is that they are linear combinations of mixtures of different ages as mentioned in the previous section. However, some data lie outside the natural domain as defined before. In figure 1, which contains data greater than 0.5 WL, there are approximately 44 data points lying outside the natural domain, and in figure 2, which contains data smaller than 0.5 WL, there are about 10 points.

Besides the spread of the data points, there are also some nonzero correlation coefficients inasmuch as the distributions of data in figures 1-2 do not have a circular shape, but rather, a curved and elongated one. At first approximation, most data are located in the vicinity of the equilibrium point.

Breslin, George, and Weinstein (1), to explain the spread and correlation of the data, used the concept of radon daughter growth models as mentioned in the "Introduction." In more detail, they are:

Model 1. An enclosed, ventilated volume with constant radon emanation. This is also called the radon chamber model.

Model 2. Continuous radon emanation with no mixing. This is also called the mine tunnel model.

Model 3. Initially pure radon concentration with no mixing as described by Evans (4).

Models 2 and 3 have no airflows passing through the volume. Model 3 is described exactly by the curve shown in figures 2-4. The times marked in minutes for various points on the curve indicate the age of air in the exact sense as defined by Evans. Models 1 and 2 fall entirely into the region defined by this curve and the straight line joining the equilibrium point and the pure RaA point which is considered the natural domain.

Growth models 1 and 2 cover an area which is entirely within the natural domain. This leads to conclusions that about 44 points lying outside this area in figure 2 and about 10 points in figure 3 cannot be explained by any of the growth models. In addition, from this discussion it follows that it is impossible to decide which growth model applies to the given data because, when mixing is allowed, there is a complete overlap of all three models. In fact, even without mixing it would be difficult to decide on a growth model because of the errors. Moreover, it is very difficult to make sure no mixing took place in a turbulent mine atmosphere.

Plateout

In this work plateout is understood as a "fast loss of airborne daughter products to mine surfaces." The main reason for singling out this phenomenon as of prime importance is that the radon daughter concentration in ventilated mines is always much lower than the parent radon concentration.[8] The two main reasons for this are the much higher chemical activity of radon daughters than for radon itself and the very high mobility of radon daughter atoms or molecules before they get attached to airborne particles.[9]

Both the previous section on radon daughter growth models and this section are concerned with the depletion of radon daughters with respect to the parent radon concentration. These depletions can be classified in the following manner:

1. Depletion according to Evans' (4) description as nonequilibrium radon, radon daughters system. In this work, following reference 1, the model is the

[8] The average WLR for the data in figures 2-3, $\simeq$ 0.3 to 0.4.

[9] Sometimes even the attached radon daughters are removed from the atmosphere by gravity or diffusion to mine surfaces and to exclude this process, the above definition uses the word fast to imply that it takes place more rapidly for uncombined radon daughters.

growth model 3. It is given in figures 1-4 as the curve starting from the lower left corner and ending at the equilibrium point.

2. Depletion according to models 1 and 2. As mentioned before, the mixtures corresponding to these models are entirely within the natural domain which was defined in the previous section. The mixtures pertinent to these models for a given WLR are indicated in figure 4 and table 1.

3. In addition to the radioactive transmutation depletions, there are plateout depletions that affect all radon daughters equally. The result of such plateout is no change in mixtures; therefore, there is no shift in location in the triangular graphs which are normalized to 1 WL.

4. Depletions of more interest are those that do not affect all the daughters equally with a resulting shift in the position on the triangular graphs. This case may result from selective plateout.

From the four points it is clear that it is very difficult to determine uniquely the sources of these depletions. To recapitulate, three aspects of these difficulties can be specified.

1. The experimental WLR does not coincide with any of the theoretical WLR's in terms of mixtures as shown in figure 4. The theoretical locations, which all have working level ratios shown in figure 4, have wide ranging ages.

2. There is no simple model, and no age, that would give the experimentally determined average WLR and the corresponding mixtures. The only way to form those mixtures would be by mixing radon daughters of various ages.

3. As mentioned before, approximately 60 data points lie outside the natural domain; these cannot be formed by mixing radon daughters of various ages. The only likely explanation is selective plateout.

The most likely daughter to plateout is RaA (the first daughter to be formed from the inert gaseous radon parent as a free and probably charged atom). As Mercer (8) states, if the RaA atom should plateout, then there is a great probability it will reenter the gas phase on recoil. The recoil energy of the now RaB atom is 112 kev; the adsorption energy is of the order of 1 ev; the RaB atom clearly has a good change of recoiling.

The net result of this sequence of events is the suppression of RaA activity relative to RaB and RaC, very much like those data points which lie outside of the natural domain in figure 2. It is tempting to state that all data points are shifted in the direction of the lower RaA region. This hypothesis is probably supported by the fact shown in figure 4 where all of the experimentally measured average working level ratios are displaced, approximately, in the direction of a lower RaA component with respect to the theoretical values.

Until now, only various average mixtures and about 60 points lying outside the natural domain have been discussed. There is, however, another noteworthy feature in figures 2 and 3, namely, the spread of the data. In view of this

discussion, it seems plausible to propose that the spread of the data is real, that it reflects the physically changing conditions which make the RaA, RaB, and RaC mixtures change. In other words, the spread of the data within and without the natural domain is not due only to the inaccuracies of the measurement methods.

The changes in surrounding conditions can be caused by the following:

1. Low or changing concentrations of condensation nuclei.

2. Changing humidity.

3. The presence of turbulence, which by its nature, can produce large differences from relatively minor changes.

4. Differently charged mine surfaces and airborne particles; these conditions influence both the working level ratios as well as the mixtures.

To check these considerations, a series of experiments were made in the Bureau's experimental uranium mine. The results are given in figure 5 which has 22 data points. The error bars, indicated for some of the data points, show the uncertainty of the counting statistics for RaA and RaB components.

Most radon daughter concentrations were about 3 WL; those that were lower are marked in figure 5. The 13 data points that are enclosed in a circle have been measured during periods when steady conditions prevailed, a condensation nuclei generator[10] running, and after the ventilation fans have been running for about 16 hours. These conditions result in data that are quite closely grouped. The rest of the data points are quite scattered. This could have happened when the diesel engine was shut off, or when the measurements were made in a closed room with markedly lower condensation nuclei concentrations and with otherwise poorly defined atmospheric conditions.

It may be concluded from this experiment that the spread of the data points in figure 5 is probably due to the changing conditions as defined previously. This conclusion has been also reached by Breslin and others (1).

Confirmation of this conclusion can also be obtained from the fact that about 200 measurements obtained in the Bureau of Mines experimental radon chamber are very tightly grouped in the same kind of plot as in figure 5.

Another important feature is that this spread of the data points has not markedly changed for the better with more advanced measurement techniques. The points indicated in figure 2 by △ are the older Lovett (6) compilation; while the points indicated by ⊡ are recent measurements taken by MESA (9). It is true that the main bulk of the data points lies somewhat lower than those compiled by Lovett (fig. 4), which means higher RaA concentration with respect to RaB and RaC, and which, in turn, suggests better ventilation; however, the spread of the data remains as wide as before which would be the case if the sources of spread described played important roles.

---

[10] A small diesel engine.

The counting statistics errors are displayed in figure 6, and the corresponding error bars in figure 5. It is very fortunate that the standard deviation for WL, σ_{WL}, the dash-dot line in figure 6, is relatively small.

For comparison, the total error for the Kusnetz method is shown. The counting time is 10 minutes, which is longer than the fieldworkers usually use; therefore, in most cases the error is worse than shown in figure 6.

In general, there is very good agreement between WL measurements using the thermoluminescent dosimeter (TLD) and the modified Tsivoglou measurements. The TLD tests have been performed in the Bureau laboratory in connection with the development of personal dosimeters. The TLD measurements operate on an energy dependent principal, while Tsivoglou depends on counting events. The agreement indicates that errors due to self-absorption for RaA and RaC' due to different alpha energies are not seriously affecting Tsivoglou measurements.

In spite of the ambiguities in the concepts of age of air and of WLR, it can be said that whatever mechanism is causing the ambiguity in associating the radon daughter mixtures with WLR and the corresponding age, the correlation between them is not totally eliminated.

CONCLUSIONS

The variations of the mixtures of RaA, RaB, and RaC are the result of unsteady conditions and selective plateout. No simple correlation with the radon daughter growth models could be found. The mixtures that fall outside the natural domain can be explained only by selective plateout. The width of the distribution is explained, except for the random and systematic errors, by the changes in the surrounding conditions. All conclusions have been reached with the aid of the two-dimensional triangular graph which is especially suited for these analyses.

REFERENCES

1. Breslin, A. J., A. C. George, and M. S. Weinstein. Investigation of the Radiological Characteristics of Uranium Mine Atmospheres. AEC-HASL Rept. 220, 1969, pp. 1-63.

2. Cooper, J. A., P. O. Jackson, J. C. Langford, M. R. Peterson, and B. O. Stuart. Characteristics of Attached Radon-222 Daughters Under Both Laboratory and Field Conditions With Particular Emphasis Upon Underground Uranium Mine Environments (Research Contract No. HO220029). BuMines Open File Rept. 57-74, 1974, 288 pp.; available for consultation at Bureau of Mines facilities in Denver, Colo., Twin Cities, Minn., Pittsburgh, Pa., and Spokane, Wash.; Department of Energy facilities in Morgantown, W. Va.; and the National Library of Natural Resources, U.S. Department of the Interior, Washington, D.C.

3. Droullard, R. F., and R. F. Holub. Continuous Working Level Measurements Using Alpha or Beta Detectors. BuMines RI 8237, 1977, pp. 1-13.

4. Evans, Robley D. Engineer's Guide to the Elementary Behavior of Radon Daughters. Health Phys., v. 17, 1969, pp. 229-252.

5. Holub, R. F., and R. F. Droullard. Evaluation of Various Radon Daughter Measurement Methods. Proc. Workshop on Methods for Measuring Radiation in and Around Uranium Mills, Albuquerque, N. Mex., May 23-26, 1977, E. D. Harvard (ed.), v. 3, No. 9, 1977, pp. 197-219; available from Atomic Industrial Forum, Inc., Washington, D.C.

6. Lovett, D. B. Investigation of the Various Factors Affecting the Response of Passive Configuration Track Etch Dosimeters to Working Level Hour Exposure (Research Contract HO232046). BuMines Open File Rept. 76-77, 1976, 167 pp.; available for consultation at Bureau of Mines facilities in Denver, Colo., Twin Cities, Minn., Bruceton and Pittsburgh, Pa., and Spokane, Wash.; Department of Energy facilities in Carbondale, Ill., and Morgantown, W. Va.; the National Library of Natural Resources, U.S. Department of the Interior, Washington, D.C.; and National Technical Information Service, Springfield, Va., PB 266 768/AS.

7. Martz, D. E., D. F. Holeman, D. E. McCurdy, and K. J. Schiager. Analysis of Atmospheric Concentrations of RaA, RaB and RaC by Alpha Spectroscopy. Health Phys., v. 17, 1969, pp. 131-138.

8. Mercer, T. T. Effect of Particle Size on the Escape of Recoiling RaB Atoms From Particulate Surfaces. Health Phys., v. 31, August 1976, pp. 173-174.

9. Rock, R. L. Private communication, 1975. Available upon request from the Mine Safety and Health Administration, Denver, Colo.

10. Rolle, R. Improved Radon Daughter Monitoring Procedure. Am. Ind. Hyg. Assoc. J., v. 30, 1969, pp. 153-160.

11. Thomas, J. W. Modification of the Tsivoglou Method for Radon Daughters in Air. Health Phys., v. 19, November 1970, pp. 691-692; Measurement of Radon Daughters in Air. Health Phys., v. 23, December 1972, pp. 783-789.

12. Wigley, T. M. L. Non-Steady Flow Through a Porous Medium and Cave Breathing. J. Geophys. Res., v. 72, June 1967, pp. 3199-3205.

☆U.S. GOVERNMENT PRINTING OFFICE: 1978-703-103/89

INT.-BU.OF MINES,PGH.,PA. 23339